

# Contact Area Design of Ohmic RF MEMS Switch for Enhanced Power Handling

Anuroop<sup>1,2</sup>

<sup>1</sup>Transducers & Actuators Group  
CSIR-Central Electronics Engineering  
Research Institute,  
Pilani, India

<sup>2</sup>Academy of Scientific and Innovative  
Research, CEERI Campus,  
Pilani, India  
anuroop@ceeri.res.in

Prem Kumar<sup>1</sup>

Transducers & Actuators Group  
CSIR-Central Electronics Engineering  
Research Institute,  
Pilani, India

Deepak Bansal<sup>1,2</sup>

<sup>1</sup>Transducers & Actuators Group  
CSIR-Central Electronics Engineering  
Research Institute,  
Pilani, India

<sup>2</sup>Academy of Scientific and Innovative  
Research, CEERI Campus,  
Pilani, India

Amit Kumar<sup>1,2</sup>

<sup>1</sup>Transducers & Actuators Group  
CSIR-Central Electronics Engineering  
Research Institute,  
Pilani, India

<sup>2</sup>Academy of Scientific and Innovative  
Research, CEERI Campus,  
Pilani, India

Khushbu<sup>1</sup>

Transducers & Actuators Group  
CSIR-Central Electronics Engineering  
Research Institute,  
Pilani, India

Kmaljit Rangra<sup>1,2</sup>

<sup>1</sup>Transducers & Actuators Group  
CSIR-Central Electronics Engineering  
Research Institute,  
Pilani, India

<sup>2</sup>Academy of Scientific and Innovative  
Research, CEERI Campus,  
Pilani, India

**Abstract**— RF MEMS switches are small in size, consume low power and have good RF response. However, the field deployment of RF MEMS switches is restricted due to limited power handling capability and reliability issues. In literature, power handling is improved through contact area either by adding hard materials or increasing the thickness. In the present paper, calculations for contact area versus stiction forces are performed and RF MEMS ohmic switch with optimal contact area is proposed and fabricated. The power handling of RF MEMS switch is increased by 55.86% without the addition of new material or processing steps. Insertion loss and return loss of the switch are also improved using corner compensation.

**Keywords**—Ohmic Switch, Power Handling, RF MEMS

## I. INTRODUCTION

Miniaturization in the wireless communication and demand of low power consumption has resulted in development of RF MEMS technology. RF MEMS devices have superior RF performance and lower power consumption compared to solid state devices. The MEMS switches in particular are basic elements in these devices like antenna, phase shifter, filters etc. Electrostatic RF MEMS switches consume almost zero power and best suited for satellite communication applications. Communication systems in satellite and radar based applications, use coaxial switches and waveguides which offer good RF behavior but have disadvantages of size and weight. RF MEMS switch is viable replacement for both solid state and co-axial system in term of RF performance and size. However, RF MEMS devices have basic limitations of reliability and low power handling which restricts its utilizations in high power applications. The power carrying capability is limited by two major factors namely: 'self-actuation' and 'electromigration'. In self-actuation, switch changes its state from 'ON' to 'OFF' or vice-versa without external biasing. Such problems prevail in the switches which have common DC and RF signals [1], [2]. Problem is solved by using separate DC and RF signals or adding pull-up electrodes[3] [4], [5]. Another solution [6] is to use additional top electrode to compensate self-

actuation problems but that requires double sacrificial and hanging structures which increases the process complexities. Floating metal [7] [8] is also used to overcome self-actuation mechanism. Power handling by self-actuation is addressed successfully and not explored in current paper.

The second component for power handling is electromigration refers to mass transport in metal when subjected to high current density. One way to tackle electromigration is to increase the thickness of the structure [9], [10] which leads to high pull-in voltage (80-90 V). Research[11]–[14] is also going on development of hard/high power handling materials to increase the power handling but that increases the contact resistance and requires additional processing. However, designing part of contact bumps is not much explored in the literature. In this paper, contact analysis to improve the power handling of RF MEMS devices is performed. The novelty of the proposed approach is that it does not require any special material development or processing cost to increase the power handling.

## II. CONTACT AREA

Most of the MEMS switches are prone to stiction[7], [15], [5], [16] and electromigration[11], [13], [14]. Magnitude of both electromigration and stiction forces are directly proportional to contact area. Decrease in contact area reduces the power handling whereas increase in contact area enhances the stiction probabilities. Therefore, contact area needs to be optimized. In order to find the optimal contact area, a comparative study of stiction and restoring forces is done as follow.

### A. Stiction Force

The failure of most of the MEMS devices is primarily due to stiction which need to be addressed. Three major stiction forces are capillary condensation, Van der Waals and electrostatic, each of which scales up with surface area as discussed below:

#### A.1. Capillary energy per unit area [17]

$$E_{cap} = \int 2\gamma \cos(\theta) h(z) dz \quad (1)$$

$z$  is roughness elevation,  $\gamma$  is the surface tension of water,  $h(z)$  is roughness distribution function and  $\theta$  is the contact angle.

A.2. Van der Waals energy per unit area [17]

$$E_{vdw} = \int \frac{A_H}{24\pi z^2} h(z) dz \quad (2)$$

$A_H$  is the Hamaker constant

A.3. Electrostatic energy per unit area [18]

$$E_{El} = \frac{\epsilon_0 \epsilon V^2}{2d} \quad (2)$$

$\epsilon$  and  $d$  are dielectric constant and thickness of oxide, and  $V$  is potential difference.

Among these forces [17], magnitude of Van-der Waals force lies in the range of 10-10 to 10-12  $\mu\text{J}/\mu\text{m}^2$  which is too small to be neglected. Electrostatic stiction is due to impurity charges in the oxide those magnitude is also small and neglected. Third and most effective stiction force is capillary force those magnitude lies in the range of  $5 \times 10^9$  to  $10^9 \mu\text{J}/\mu\text{m}^2$  at relative humidity of 30-60%. The estimation of optimal contact area is done based on capillary and restoring force.

### B. Restoring Energy

Restoring force of the mechanical device is determined in term of structural stiffness which is function of spring constant given by

$$E_R = \frac{kx^2}{2} \quad (3)$$

$k$  is spring constant, and  $x$  is displacement of the beam.

For the given structure,  $x=2 \mu\text{m}$

And  $k = 0.4 \text{ N/m}$  from simulations performed on Coventorware.

Hence maximum restoring energy  $E_R = 0.8 \times 10^{-6} \mu\text{J}$ .

For 60% humidity, maximum possible contact area is given by

$$\text{Area} = \frac{0.8 \times 10^{-6}}{5 \times 10^{-9}} = 160 \mu\text{m}^2$$

Be on safer side, contact area close to  $140 \mu\text{m}^2$  is chosen.

### III. CONTACT AREA OPTIMIZATION

Bumps are made at contact area to prevent stiction and most of the bumps are square and circular in shape [11], [13], [14], [24], [25]. However, sharp corners in square bump results in high current density which lower the power handling (power handling is directly proportional to square of the current). In order to avoid sharp corners, circular bumps are proposed [26] which handles more power. Based

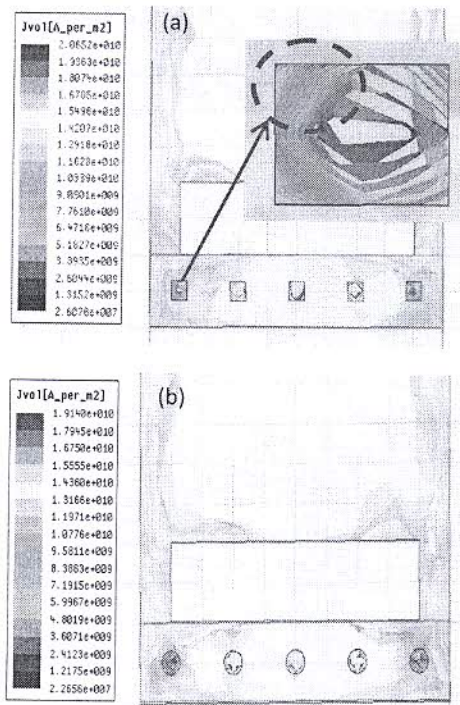


Fig. 1. Bump current density distribution of RF MEMS switch for (a) square, (b) circular shapes

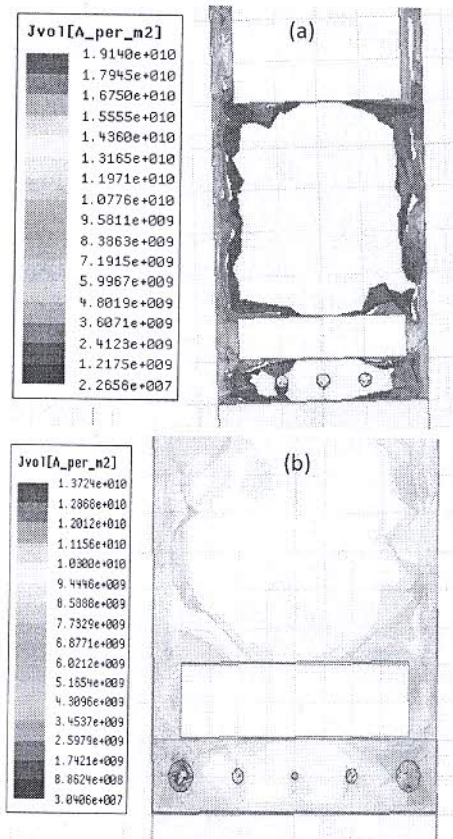


Fig. 2. (a) Current flow distribution across the cantilever switch with uniform circular bump and (b) modified circles in hourglass arrangement.

on current distributions as shown in Figure 1, current density at circular bumps is decreased by 7.27% compared to square bumps which leads to 13.85% higher power handling. As, most of current flows across edges of the switch as shown in Figure 2 (a), bumps from central part of the structure can be removed. However, central support is required for mechanical stability to keep the structure tip straight. Hence, we have proposed non-uniform bumps across the switch in hourglass manner as shown in Figure 2 (b). Total contact area is kept close to  $140 \mu\text{m}^2$  as shown in Figure 3. The radius of the circular bumps is increased from  $1 \mu\text{m}$  at center to  $2 \mu\text{m}$  in middle and  $4.25 \mu\text{m}$  at edge. Hourglass shaped bumps have 28.33% lower current density as compared to uniform circular bump which leads to 48.77% higher power handling. On comparing with square bumps, hourglass shaped bumps have 55.86% more power handling capability.

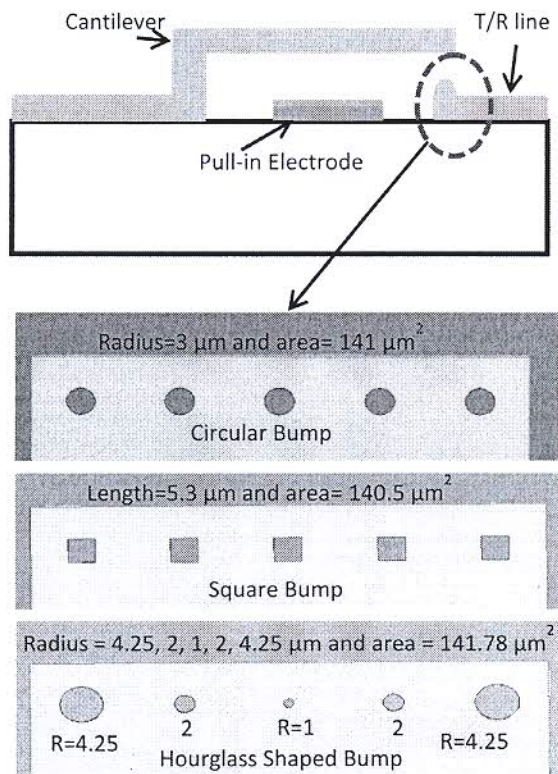


Fig. 3. RF MEMS ohmic switch with contact area and dimensions for circular, square and hourglass patterned bumps.

#### IV. FABRICATION OF PROPOSED SWITCH

Fabrication process flow of ohmic contact switch is shown in Figure 4. High resistive silicon wafer is used as the substrate material.  $\text{SiO}_2$  layer of  $1 \mu\text{m}$  thickness is thermally grown using dry-wet-dry thermal oxidation process. Polysilicon deposited by Low Pressure Chemical Vapor Deposition (LPCVD) is used as actuation electrode and base material for bumps shown in Figure 4(a). Optical images of hour glass shaped bumps base are shown in Figure 5, due to over etching center bumps is etched. Gold is sputtered over the bump area and extended outside the top cantilever called under pass area shown in Figure 4(b). In Figure 4 (c),  $\text{SiO}_2$  is deposited using Plasma-Enhanced Chemical Vapor

Deposition (PECVD) to cover the actuation electrodes to avoid shorting with the cantilever. Fujifilm HiPR 6500 is spin coated and patterned to make the sacrificial layer and followed by seed layer deposition shown in Figure 4(d).  $2 \mu\text{m}$  thick cantilever beam made by gold electroplating method shown in Figure 4(e). In order to release the cantilever structure, sacrificial layer is removed by using wet release method discussed in [27] shown in Figure 4(f). SEM micrograph of the fabricated ohmic RF MEMS switch with square bumps and circular bumps are shown in Figure 6(a) & 6(b) and hour glass shaped bumps is shown in Figure 6(c) & 6(d). Due to over etching, center bumps of the hourglass structure are etched. Most of the current flows in the edges of the cantilever beam shown in Figure 2, so etching of center bump will not affect the performance of RF MEMS switch too much.

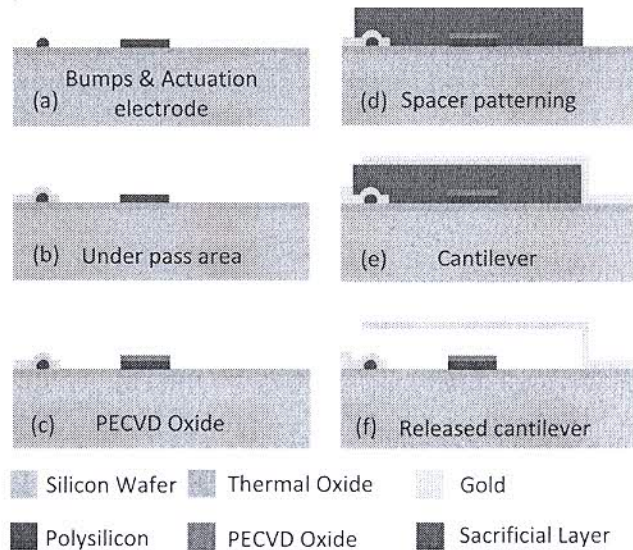


Fig. 4. Fabrication process flow of RF MEMS ohmic switch.

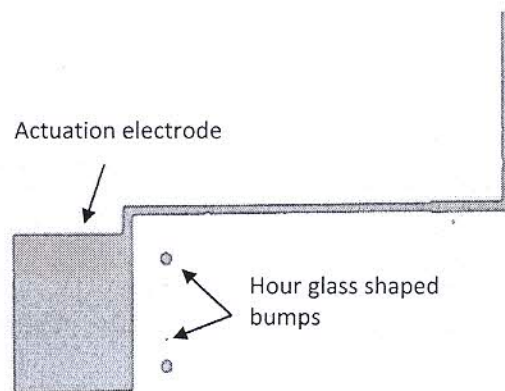


Fig. 5. Optical images of hour glass shaped bumps base

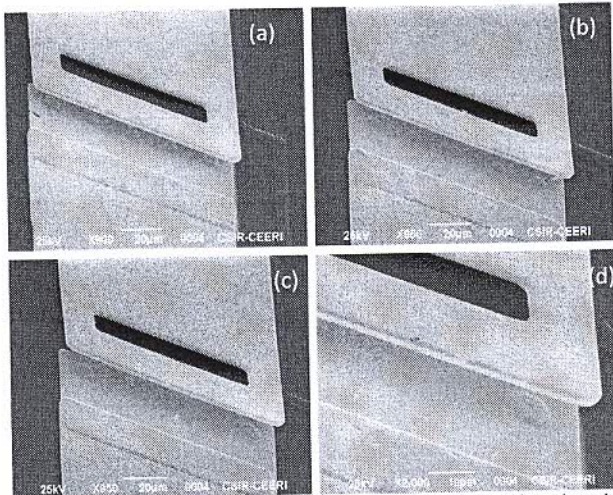


Fig. 6. (a) Square bumps (b) Circular bumps (c) & (d) Hourglass shaped bumps

## V. CHARACTERIZATION

Electromagnetic characterizations of the RF MEMS ohmic switch are performed on High Frequency Structure Simulator (HFSS). Response of the switch is better than solid state counterparts. Due to sharp corner, response of the switch with square shaped bumps is inferior compared to others configuration. However, insertion loss and isolation of the switch is better than 0.06 dB and 20 dB respectively for DC to 15 GHz as shown in Figure 7. Return loss of the switch is more than 40 dB for all the cases.

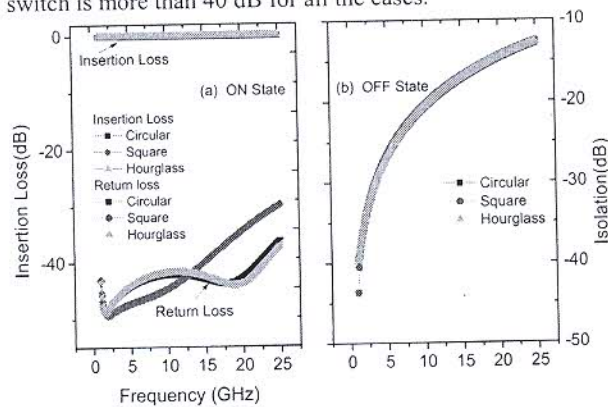


Fig. 7. 'ON' state (a) insertion, return loss and 'OFF' state (b) isolation of the switch.

## VI. CONCLUSION

A novel configuration of bump for RF MEMS ohmic switch shape is designed, fabricated and tested. Optimal contact area is selected based on stiction and restoring force which comes out to be  $160 \mu\text{m}^2$  for selected switch. Power capacity the switch is increased by 55.86% without adding any material or fabrication step. Insertion loss, return loss and isolation of the switch are better than 0.06 dB, 40 dB and 20 dB respectively for DC to 15 GHz applications.

## ACKNOWLEDGMENT

The authors would like to thanks Council of Scientific

and Industrial Research, India for providing financial assistance under SRF-Direct Scheme and MLP-105.

## REFERENCES

- [1] C. Goldsmith, T.-H. L. T.-H. Lin, B. Powers, W.-R. W. W.-R. Wu, and B. Norvell, "Micromechanical membrane switches for microwave applications," *Proc. 1995 IEEE MTT-S Int. Microw. Symp.*, pp. 91–94, 1995.
- [2] C. L. Goldsmith, Z. Yao, S. Eshelman, and D. Denniston, "Performance of Low-Loss RF MEMS Capacitive Switches," *IEEE Microw. Guid. Wave Lett.*, vol. 8, no. 8, pp. 269–271, 1998.
- [3] W. A. De Groot, J. R. Webster, D. Felhofer, and E. P. Gusev, "Review of device and reliability physics of dielectrics in electrostatically driven MEMS devices," *IEEE Trans. Device Mater. Reliab.*, vol. 9, no. 2, pp. 190–202, 2009.
- [4] K. Rangra, B. Margesin, L. Lorenzelli, F. Giacomozzi, C. Collini, M. Zen, G. Soncini, L. del Tin, and R. Gaddi, "Symmetric toggle switch—a new type of rf MEMS switch for telecommunication applications: Design and fabrication," *Sensors Actuators A Phys.*, vol. 123–124, pp. 505–514, 2005.
- [5] D. Bansal, A. Kumar, A. Sharma, and K. J. Rangra, "Design of compact and wide bandwidth SPDT with anti-stiction torsional RF MEMS series capacitive switch," *Microsyst. Technol.*, vol. 21, no. 5, pp. 1047–1052, 2015.
- [6] D. Peroulis, S. P. Pacheco, and L. P. B. Katehi, "RF MEMS switches with enhanced power-handling capabilities," *IEEE Trans. Microw. Theory Tech.*, vol. 52, no. 1, pp. 59–68, 2004.
- [7] D. Bansal, A. Bajpai, P. Kumar, A. Kumar, M. Kaur, and K. Rangra, "Design and fabrication of a reduced stiction radio frequency MEMS switch," *J. Micro/Nanolithography, MEMS, MOEMS*, vol. 14, no. 3, p. 35002, 2015.
- [8] F. Solazzi, C. Palego, D. Molinero, P. Farinelli, S. Colpo, J. C. M. Hwang, B. Margesin, and R. Sorrentino, "High-power high-contrast RF MEMS capacitive switch," *Microw. Integr. Circuits Conf. (EuMIC), 2012 7th Eur.*, pp. 32–35, 2012.
- [9] H. Zareie and G. M. Rebeiz, "High-power RF MEMS switched capacitors using a thick metal process," *IEEE Trans. Microw. Theory Tech.*, vol. 61, no. 1, pp. 455–463, 2013.
- [10] C. D. Patel and G. M. Rebeiz, "RF MEMS metal-contact switches with mN-contact and restoring forces and low process sensitivity," *IEEE Trans. Microw. Theory Tech.*, vol. 59, no. 5, pp. 1230–1237, 2011.
- [11] J. Dhennin, "Characterization of gold/gold, gold/ruthenium, and ruthenium/ruthenium ohmic contacts in MEMS switches improved by a novel methodology," *J. Micro/Nanolithography, MEMS, MOEMS*, vol. 9, no. 4, p. 41102, 2010.
- [12] R. a Coutu, P. E. Kladitis, K. D. Leedy, and R. L. Crane, "Selecting metal alloy electric contact materials for MEMS switches," *J. Micromechanics Microengineering*, vol. 14, no. 8, pp. 1157–1164, 2004.
- [13] A. Broue, T. Fourcade, J. Dhennin, F. Courtade, P. Charvet, P. Pons, X. Lafontan, and R. Plana, "Validation of bending tests by nanoindentation for micro-contact analysis of MEMS switches," *J. Micromechanics Microengineering*, vol. 20, no. 8, p. 85025, 2010.
- [14] F. Ke, J. Miao, and J. Oberhammer, "A ruthenium-based multimetal-contact RF MEMS switch with a corrugated diaphragm," *J. Microelectromechanical Syst.*, vol. 17, no. 6, pp. 1447–1459, 2008.
- [15] W. Ashurst, "Wafer level anti-stiction coatings for MEMS," *Sensors Actuators A Phys.*, vol. 104, no. 3, pp. 213–221, 2003.
- [16] R. Maboudian, W. R. Ashurst, and C. Carraro, "Self-assembled monolayers as anti-stiction coating for MEMS: characteristics and recent progress," *Sensors, Actuators A, Phys.*, vol. 82, pp. 219–223, 2000.
- [17] W. M. Van Spengen, R. Puers, and I. De Wolf, "On the physics of stiction and its impact on the reliability of microstructures," *J. Adhes. Sci. Technol.*, vol. 17, no. 4, pp. 563–582, 2003.
- [18] G. M. Rebeiz, "RF MEMS Theory, Design, and Technology," book, p. A JOHN WILEY & SONS PUBLICATION, New Jersey, 2003.
- [19] J. R. Black, "Electromigration failure modes in aluminum metallization for semiconductor devices," *Proc. IEEE*, vol. 57, no. 9, pp. 1587–1594, 1969.
- [20] I. C. Reines and G. M. Rebeiz, "A robust high power-handling (> 10 W) RF MEMS switched capacitor," *Proc. IEEE Int. Conf. Micro Electro Mech. Syst.*, pp. 764–767, 2011.

- [21] J. Xu, X. Y. Zhang, S. Member, I. J. Chen, and Q. Xue, "Filtering Switch with Low ON - State Loss and High OFF - State Isolation Based on Dielectric Resonator," pp. 1-9, 2017.
- [22] G. Jerke and J. Lienig, "Hierarchical Current-Density Verification in Arbitrarily Shaped Metallization Patterns of Analog Circuits," *IEEE Trans. Comput. Des. Integr. Circuits Syst.*, vol. 23, no. 1, pp. 80-90, 2004.
- [23] D. Bansal, A. Kumar, A. Sharma, P. Kumar, and K. J. Rangra, "Design of novel compact anti-stiction and low insertion loss RF MEMS switch," *Microsyst. Technol.*, vol. 20, no. 2, pp. 337-340, 2013.
- [24] N. E. McGruer, G. G. Adams, L. Chen, Z. J. Guo, and Y. Du, "Mechanical, Thermal, and Material Influences on Ohmic-Contact-Type MEMS Switch Operation," in *19th IEEE International Conference on Micro Electro Mechanical Systems*, 2006, no. January, pp. 230-233.
- [25] Z. J. Guo, N. E. McGruer, and G. G. Adams, "Modeling, simulation and measurement of the dynamic performance of an ohmic contact, electrostatically actuated RF MEMS switch," *J. Micromechanics Microengineering*, vol. 17, no. 9, pp. 1899-1909, 2007.
- [26] P. Jhanwar, D. Bansal, S. Pandey, S. Verma, and K. J. Rangra, "Design aspect of high power handling applications: metal contact switches," *Microsyst. Technol.*, vol. 21, no. 10, pp. 2083-2087, 2014.
- [27] A. Sharma, P. Jhanwar, D. Bansal, A. Kumar, M. Kaur, S. Pandey, P. Kumar, D. Kumar, and K. Rangra, "Comparative study of various release methods for gold surface micromachining," *J. Micro/Nanolithography, MEMS, MOEMS*, vol. 13, no. 1, p. 13005, 2014.